Chemical Science

ROYAL SOCIETY OF CHEMISTRY

EDGE ARTICLE

View Article Online
View Journal | View Issue



Cite this: *Chem. Sci.*, 2025, **16**, 2004

All publication charges for this article have been paid for by the Royal Society of Chemistry

Received 19th May 2024
Accepted 3rd December 2024

DOI: 10.1039/d4sc03269a

rsc.li/chemical-science



# Aerobic oxidation of alkylarenes and polystyrene waste to benzoic acids *via* a copper-based catalyst†

Enjie Xu, Tianwei Liu, Fuyu Xie, Jianghua He* and Yuetao Zhang *

The chemical recycling of polystyrene (PS) waste to value-added aromatic compounds is an attractive but formidable challenge due to the inertness of the C–C bonds in the polymer backbone. Here we develop a light-driven, copper-catalyzed protocol to achieve aerobic oxidation of various alkylarenes or real-life PS waste to benzoic acid and oxidized styrene oligomers. The resulting oligomers can be further transformed under heating conditions, thus achieving benzoic acid in up to 65% total yield through an integrated one-pot two-step procedure. Mechanistic studies show that the $CuCl_2$ catalyst undergoes Ligand-to-Metal Charge Transfer (LMCT) to generate a chlorine radical, which triggers activation of the C–H bond and subsequent oxidative cleavage of C–C bonds. The practicality and scalability of this strategy are demonstrated by depolymerization of real-life PS foam on a gram scale, thus showing promising application potential in chemical recycling of PS waste.

## Introduction

Polystyrene (PS), one of the most manufactured plastics in the world, exhibits wide applications in various fields, such as packaging, thermal insulation and electronics. The annual production of PS is estimated to be nearly 17 million tons per year.[1] However, end-of-life PS plastics either become landfill waste or escape into the environment, which not only aggravates ecological distress but also threatens human health.[2–4] Although progress has been made in the development of methods to recover end-of-life polymers,[5–15] the PS recycling rate remains below 1%.[16,17] As one of the most valuable all recycling methods, chemical recycling has demonstrated promising potential in the depolymerization of these post-consumer polymer products into useful chemical feedstocks.[18,19] However, it remains formidably challenging to realize chemical recycling of PS waste due to the inertness of C–C bonds in the polymer backbone.[20,21] Research efforts have continuously focused on the traditional thermal depolymerization of PS (Scheme 1A). For example, the chemical oxidation of PE, PP and PS to organic acids was achieved by the Co(II)/Mn(II) system at 150–210 °C,[22–24] the oxidative depolymerization of PS into benzoic acid was obtained by nitric acid at 180 °C.[25] Yan and co-workers reported the reductive upcycling of various aromatic plastic waste (PET, PS, PPO, and PC) to arenes through catalytic hydrogenolysis over a $Ru/Nb_2O_5$ catalyst at 320 °C and 0.5 MPa $H_2$.[26] Jiao *et al.* utilized organic azide to synthesize arylamines from alkylarenes and PS with the catalysis of $FeCl_2$,[27] while Liu's group developed a "degradation-upcycling" strategy for the synthesis of aryl ketones and organosulfur compounds from PS waste in the presence of equivalent $AlCl_3$.[28] Despite the efficiency of existing thermal methods, the requirement of high temperatures restricts their practical application in industry.

Compared with thermal catalysis, photocatalysis has emerged as a powerful and sustainable method that exhibits unique reactivity under mild conditions.[29,30] Intense interest has been focused on the photochemical oxidation degradation

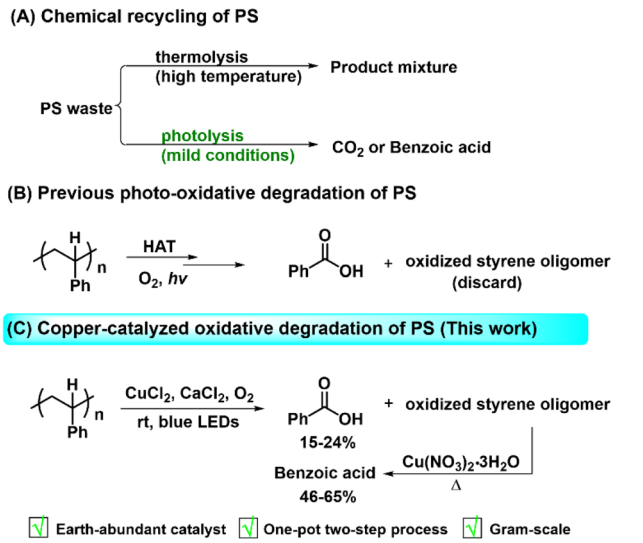


Scheme 1 (A) Chemical recycling of PS; (B) previous studies on the photo-oxidative degradation of PS; (C) copper-catalyzed oxidative degradation of PS (this work).

*State Key Laboratory of Supramolecular Structure and Materials, College of Chemistry, Jilin University, Changchun, Jilin, 130012, China. E-mail: hjh2015@jlu.edu.cn; ytzhang2009@jlu.edu.cn*

† Electronic supplementary information (ESI) available. See DOI: https://doi.org/10.1039/d4sc03269a

of PS due to the use of visible light irradiation and the inexpensive oxidant of oxygen.[31–33] The oxidative degradation of PS involves C–H bond activation and subsequent oxidation with $O_2$ to facilitate the formation of an organic peroxide, leading to the cleavage of the C–C bond and the generation of oxidized products in the end (Scheme 1B).[34] Zhu's group developed a non-selective process for photooxidation of PS plastic into $CO_2$ *via* the copper phthalocyanine sensitized $TiO_2$ photocatalyst under fluorescent light,[35] along with the production of $CO_2$. Recently, progress has been made in the photocatalytic oxidative deconstruction of PS into value-added benzoic acid. It was reported that the chlorine radical generated from $FeCl_3$ (ref. 36–39) or the catalytic system of acridinium salts and HCl[40] facilitated abstraction of hydrogen atoms from the PS backbone and subsequent oxidation, resulting in formation of benzoic acid as a major product along with oligomers. It has been demonstrated that the reactive oxygen species could initiate PS degradation into benzoic acid under photo irradiation by an acid-catalyzed strategy at room temperature[41,42] or heterogeneous graphitic carbon nitrides at 150 °C.[43] Reisner *et al.* utilized fluorenone as a direct HAT agent in combination with 1 equivalent of $H_2SO_4$ as an acidic additive to realize the depolymerization of PS to benzoic acid (30%), other aromatic compounds (20%) and oligomers.[44] By using an anthraquinone photocatalyst, Kokotos *et al.* discovered that the aerobic oxidation of PS plastics afforded benzoic acid in 25–58% yields, without requirement of acidic additive.[45] Das and co-workers reported the photocatalyst system of NBS and $CF_3SO_2Na$ for selective upcycling of real-life PS-based waste into benzoic acid, which can be further transformed into valuable aromatics.[46] The photooxidative degradation of plastic waste (PS *etc.*) into commercial chemicals was achieved *via* V(O)(acac)$_2$ (ref. 47) or $UO_2(NO_3)_2 \cdot 6H_2O$.[48] So far, it remains greatly challenging to obtain a single product in high yield due to the poor product selectivity and formation of the oxidized oligomer waste by the current strategies. Therefore, it is in high demand to develop a more efficient and cost-effective degradation strategy to produce a target compound from real-life plastic waste.

Earth-abundant Cu-based photocatalysts have been employed in visible light photocatalysis for production of valuable chemicals in an ecologically friendly and cost-effective manner.[49–53] It is known that $CuCl_2$ is capable of serving as a visible-light photocatalyst and the photoinduced ligand dissociation of $CuCl_2$ complex generates CuCl and the chlorine radical through ligand-to-metal charge transfer (LMCT).[54–58] The formation of the chlorine radical provides the opportunities to realize the challenging chemical transformations. For instance, Wan's group developed a $CuCl_2$-promoted photocatalytic strategy to realize the vicinal dichlorination of alkenes and styrenes in the presence of HCl.[59] Rovis's group reported the $CuCl_2$-catalyzed alkylation of alkanes with electron-deficient olefins.[60] Encouraged by these pioneering works, we also applied this photocatalytic LMCT strategy to the generation of chlorine radicals for the abstraction of the C–H bond from the polymer backbone under mild conditions. Besides, chlorine radicals are widely used as hydrogen abstraction agents due to their characteristic electrophilic selectivity towards the strong electron-rich C–H bonds ($\Delta H_{diss}$(HCl) = 103 kcal mol$^{-1}$),[61] and are kinetically matched with the more hydridic C–H bonds of the polymer backbone.[36–38] In this context, we developed a practical copper-based photocatalytic system consisting of readily available $CuCl_2$ as a LMCT reagent, $CaCl_2$ as a chlorine source and $O_2$ as a terminal oxidant, which enabled the oxidative cleavage of a wide range of alkylarene and real-life PS waste to benzoic acid and oxidized styrene oligomers (Scheme 1C). The corresponding oligomers can be further transformed under heating conditions, thus achieving benzoic acid in up to 65% total yield in a one-pot two-step manner.

# Experimental

### Materials and methods

All reagents were used as received unless otherwise noted. $CuCl_2$ was purchased from Energy Chemical. $CaCl_2$ powder was purchased from Beijing Chemical Works. The methanol and MeCN (HPLC grade) were purchased from Sigma-Aldrich. Reactions were monitored by thin layer chromatography (TLC), visualizing with ultraviolet light (UV); column chromatography purifications were carried out using silica gel. The reaction mixture was analyzed by a Waters High Performance Liquid Chromatograph (HPLC) system equipped with an autosampler, a C18 column (length: 150 mm, internal diameter: 4.6 mm, 35 °C) and UV/vis detector ($\lambda$ = 220 nm). $CH_3OH$: 0.1% HCOOH in $H_2O$ was used as a mobile phase with a flow rate of 1.0 mL min$^{-1}$. $^1$H NMR spectra was recorded on a Bruker Avance II 500 (500 MHz, $^1$H) instrument at room temperature (rt). Chemical shifts ($\delta$) were reported as parts per million (ppm). The number-average molecular weight ($M_n$) and molecular weight distributions (PDI = $M_w/M_n$) of PS were measured by gel permeation chromatography (GPC) at 40 °C and a flow rate of 1 mL min$^{-1}$, using THF (HPLC grade) as an eluent on a Waters 1515 instrument equipped with a Waters 4.6 × 30 mm guard column and three Waters WAT054466, WAT044226, and WAT044223 columns. The instrument was calibrated with PS standards, and chromatograms were processed with Waters Breeze2 software.

### General procedure for light-induced catalytic reactions

**The general procedure for the photooxidative reaction of alkylarenes.** A 10 mL Schlenk tube with a screw cap was charged with substrate (0.1 mmol, 1 eq.), $CuCl_2$ (5 mol%), $CaCl_2$ (20 mol%), and 1.0 mL MeCN. An oxygen balloon was equipped to maintain an oxygen atmosphere and the whole reaction tube was kept for 24–72 h under the irradiation of two Kessil H150B 50 W blue LEDs lamps at room temperature (*ca.* 25 °C), using an electric fan to control the temperature. After the reaction, the resulting mixture was dissolved with MeOH to constant volume in a 10 mL volumetric flask and then filtered. The filtrate was measured by HPLC equipped with an autosampler.

**The general procedure for the photooxidative degradation of PS.** A 10 mL Schlenk tube with a screw cap was charged with PS waste (0.1 mmol, 10.4 mg), $CuCl_2$ (5 mol%), $CaCl_2$ (20 mol%) and MeCN/benzene (0.3 mL/0.3 mL). The reaction mixture was

stirred for 5 min in the dark. Then an oxygen balloon was equipped to keep the oxygen atmosphere and the whole reaction tube was kept for 24 h under the irradiation of two Kessil H150B 50 W blue LEDs lamps at room temperature, using an electric fan to control the temperature. After the reaction, the resulting mixture was dissolved with MeOH to constant volume in a 5 mL volumetric flask and then filtered with a PTFE syringe filter. The filtrate was measured by HPLC equipped with an autosampler.

**The general procedure for the oxidative degradation of PS *via* a two-step one pot process.** First step: a 10 mL Schlenk tube with a screw cap was charged with PS waste (0.1 mmol, 10.4 mg), $CuCl_2$ (5 mol%), $CaCl_2$ (20 mol%) and MeCN/Benzene (0.3 mL/0.3 mL). The reaction mixture was stirred for 5 min in the dark. Then an oxygen balloon was equipped to maintain an oxygen atmosphere and the whole reaction tube was kept for 24 h under the irradiation of two Kessil H150B 50 W blue LEDs lamps at room temperature, using an electric fan to control the temperature. Second step: after the first step, $Cu(NO_3)_2 \cdot 3H_2O$ (20 mol%), and MeCN (1 mL) were added into the mixture obtained in the first step, and then the mixture was degassed and exchanged with $O_2$. Next, the mixture was sealed in a pressure tube and heated at 140 °C for 24 h, and then cooled down to room temperature after reaction. The resulting mixture was dissolved with MeOH to a constant volume in a 5 mL volumetric flask and then filtered with a PTFE syringe filter. The filtrate was measured by an HPLC equipped with an autosampler.

## Results and discussion

Previously, PS degradation strategies were reported to be adapted from the strategy for cleavage of C–C bonds in small molecules.[44] Therefore, we initially optimized the reaction condition for the oxidative C–C bonds cleavage of propylbenzene (**1u**) to benzoic acid (**2a**) by using a copper-based catalyst in $O_2$ atmosphere with the irradiation of blue light (Table 1). The employment of $CuCl_2$ led to the production of **2a** in 40% yield (entry 1, Table 1), whereas other non-chloride copper salts such as $Cu(OAc)_2 \cdot H_2O$, $Cu(NO_3)_2 \cdot 3H_2O$ and $CuSO_4 \cdot 5H_2O$ were ineffective for this reaction in up to 24 h (entries 2–4, Table 1), highlighting the essentially important role of the chlorine radicals generated from $CuCl_2$ for this reaction. Previously, photoactive species $CuCl_3^-$ generated from the addition of exogenous chloride was found to facilitate the chlorine radical formation and C–H abstraction.[60] Notably, metal chloride has a dual role in serving as a chlorine source of $CuCl_2$ and modulating the activity of the copper-oxo intermediates ($Cu^{II}$-O-O and $Cu^{II}$-O) by the Lewis acidity of the metal ion,[62] especially the latter has a predominant effect. The addition of LiCl, $MgCl_2$ or $CaCl_2$ can significantly enhance the yields of **2a** to 67%, 72% or 75%, respectively (entries 5–7, Table 1), while there was no improvement effect exhibited by HCl, NaCl, KCl or $SrCl_2$ due to their weak Lewis acidity[63–65] (entries 8–11, Table 1). The employment of CuCl also showed high efficiency, leading the good yield of **2a** in 63% (entry 12, Table 1). Literature research revealed that the bromine radicals generated from $CuBr_2$ under photoexcitation could also abstract hydrogen atoms.[66] However, using $CuBr_2$ instead of $CuCl_2$, drastically decreased the yield of **2a** (entry 13, Table 1). The addition of bromine additives to the reactions catalyzed by $CuBr_2$ only slightly increased the yield of **2a** to 27% (entry 14, Table 1). Switching back to $CaCl_2$ could maintain the high yields of **2a** by using $CuBr_2$ or CuBr catalyst (66% for entry 15 and 63% for entry 16, Table 1), highlighting the importance of $CaCl_2$ in achieving **2a** in high efficiency. Reducing the concentration of $CuCl_2$ (1 mol%) or $CaCl_2$ (10 mol%) decreased the yield of **2a** to 40% or 69%, respectively (entries 17 and 18, Table 1). Irradiation of the reaction with 30 W blue LEDs furnished **2a** in 63% yield whereas 71% yield of **2a** was obtained in the air (entries 19 and 20, Table 1). Control experiments showed that without $CuCl_2$, light or $O_2$, there is no observation of **2a** in 24 h, demonstrating the indispensable role of these factors for this reaction (entries 21–23, Table 1). We also screened the effectiveness of different solvents on this reaction (*i.e.* MeOH, THF, DCM, EtOAc, acetone and DMF) (Table S1†) and found that acetonitrile showed the best performance, probably due to the stabilization of copper complexes through the ligation of nitrile to copper.[55]

Table 1 Optimization of the photooxidative cleavage of C–C bond in propylbenzene (**1u**)[a]

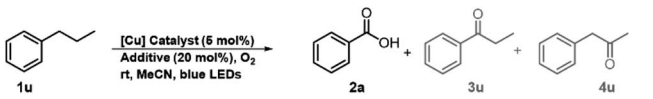


| Entry | [Cu] catalyst | Additive | Yield (%) 2a | 3u | 4u |
|---|---|---|---|---|---|
| 1 | $CuCl_2$ | None | 40 | 14 | 9 |
| 2 | $Cu(OAc)_2 \cdot H_2O$ | None | 0 | 0 | 0 |
| 3 | $Cu(NO_3)_2 \cdot 3H_2O$ | None | 0 | 0 | 0 |
| 4 | $CuSO_4 \cdot 5H_2O$ | None | 0 | 0 | 0 |
| 5[b] | $CuCl_2$ | LiCl | 67 | 6 | 8 |
| 6 | $CuCl_2$ | $MgCl_2$ | 72 | 1 | 6 |
| 7 | $CuCl_2$ | $CaCl_2$ | 75 | 0 | 0 |
| 8[b] | $CuCl_2$ | HCl | 40 | 3 | 2 |
| 9[b] | $CuCl_2$ | NaCl | 36 | 11 | 10 |
| 10[b] | $CuCl_2$ | KCl | 31 | 8 | 8 |
| 11 | $CuCl_2$ | $SrCl_2$ | 31 | 8 | 6 |
| 12 | CuCl | $CaCl_2$ | 63 | 3 | 0 |
| 13 | $CuBr_2$ | None | <1 | 2 | 4 |
| 14 | $CuBr_2$ | $CaBr_2$ | 27 | 0 | 1 |
| 15 | $CuBr_2$ | $CaCl_2$ | 66 | 0 | 0 |
| 16 | CuBr | $CaCl_2$ | 63 | 5 | 0 |
| 17[c] | $CuCl_2$ | $CaCl_2$ | 40 | 8 | 4 |
| 18[d] | $CuCl_2$ | $CaCl_2$ | 69 | 1 | 0 |
| 19[e] | $CuCl_2$ | $CaCl_2$ | 63 | 2 | 1 |
| 20[f] | $CuCl_2$ | $CaCl_2$ | 71 | 2 | 0 |
| 21 | — | $CaCl_2$ | 0 | 0 | 0 |
| 22[g] | $CuCl_2$ | $CaCl_2$ | 0 | 0 | 0 |
| 23[h] | $CuCl_2$ | $CaCl_2$ | 0 | 0 | 0 |

[a] Standard conditions: **1u** (0.1 mmol), $CuCl_2$ (5 mol%), $CaCl_2$ (20 mol%), MeCN (1.0 mL), $O_2$ balloon, 50 W blue LEDs, rt, 24 h. The yields were measured by HPLC using a standard curve of standard substances as reference. [b] MCl (40 mol%). [c] $CuCl_2$ (1 mol%). [d] $CaCl_2$ (10 mol%). [e] 30 W. [f] In air. [g] 80 °C in the dark. [h] In $N_2$.

With the optimized reaction conditions in hand, we examined the generality for the deep oxidation of alkylarenes (Scheme 2). It turned out that this reaction works for methylarenes with neutral (H **1a**), electron-donating (phenyl **1b** and acetoxy **1c**) or electron-withdrawing groups (acetyl **1d**; –CN **1e**; –$CF_3$ **1f**; and –Cl **1g**), furnishing the corresponding aromatic acids in good to excellent yields (68–97%). It is noted that the methylarenes with fluoride substituted at the *ortho*- (**1h**), *meta*- (**1i**), and *para*-positions (**1j**) furnished the desired products in 72–73% yields. Prolonging the reaction time to 72 h led to the smooth oxidization of 4-OH substituted methylarene (**1k**) into 4-hydroxybenzoic acid (**2k**) in 72% yield, leaving the hydroxyl group for post modifications.[67] Unfortunately, this strategy was not applicable to the $NH_2$-substituted methylarene (**1l**), probably due to the deactivation of the catalyst resulting from the coordination of $NH_2$ groups with copper. A control experiment was performed by using propylbenzene as substrates, adding one equiv. of aniline completely quenched the reaction, thus confirming the above assumption (Scheme S1a†). By using the alkylarenes with secondary benzylic C–H bonds as substrates, we further examined this photocatalytic oxidative cleavage of C–C bond (**1m–1x**). The ethylbenzene derivatives (**1m–1o**) produced the corresponding acetophenones (**3m–3o**) as major products and benzoic acid as minor products. Moreover, there was no conversion of acetophenone under photocatalytic conditions, while the oxidative cleavage of other ketone substrates into aromatic acids occurred (Scheme S2†) as acetophenone is more difficult to transform into the enol form than other ketone intermediates.[36,68] Remarkably, the strategy can be applied to the phenylethanol derivatives (**1p–1t**), delivering the corresponding benzoic acids in moderate to high yields (59–81%). The propylbenzene with a substituent on the benzene ring (**1u–1x**) produced the corresponding benzoic acids in 68–79% yields, except **1x** with the 4-OH group only afforded **2k** in 30% yield. The low efficiency might result from the inhibition of free radicals by the phenol group.

To verify this assumption, we conducted a control experiment by using propylbenzene as a substrate and found that one equiv. of phenol led to the conversion of propylbenzene drastically decreasing to 49%, furnishing propiophenone (**3u**, 10%), 1-phenylpropan-2-one (**4u**, 5%) and benzaldehyde (**7**, 10%), rather than benzoic acid (Scheme S1b†). The cumene (**1y**) and *tert*-butylbenzene (**1z**) generated acetophenones in 53% and 52% yields, respectively. All these results clearly demonstrated the good versatility of this photocatalytic strategy towards the oxidative cleavage of C–C bonds.

Encouraged by such highly efficient $CuCl_2$-catalyzed photooxidative transformation of alkylarenes into benzoic acids, we further investigated degradation of commercial PS ($M_n$ = 87 kg $mol^{-1}$, PDI = 3.29; Fig. S3†). Due to the poor solubility of PS in MeCN, we did not detect any small molecular products (Table S2†). In order to improve the solubility of PS in solvent, we investigated the cosolvent effects and found that in MeCN/benzene, high molecular weight PS could be efficiently degraded to small molecular aromatics (benzoic acid (**2a**) in 22% yield; 1,3-diphenylpropanetrione (**5**) in 3% yield; phenyl glyoxylic acid (**6**) in 6% yield, Scheme 3), the oxidized oligomers ($M_n$ = 0.11 kg $mol^{-1}$, PDI = 3.81; Fig. S3†) along with unidentified products in 24 h (Fig. S4†), respectively. Small amounts of aromatic products were detected with the cosolvents of acetone, THF, EtOAc or DCM (Table S2†).

Control experiments showed that in the presence of $CuCl_2$/$CaCl_2$ and under irradiation of blue LEDs, PS could be degraded to **2a** in 22% yield (entry 1, Table 2). Similar results were obtained with the prolonged reaction time to 36 h or heating the reaction mixture obtained from the photocatalytic first step at 120 °C for 12 h as the second step (entries 2 and 3, Table 2). The addition of $Cu(NO_3)_2 \cdot 3H_2O$ after the first step and irradiation during the second step still did not show any improvement, while the high temperature (120 °C)[69] instead of irradiation during the second step enhanced the yield of **2a** to 37% after 12 h, further up to 42% for 24 h (entries 4–6, Table 2). Replacing $CuCl_2$ with $Cu(NO_3)_2 \cdot 3H_2O$ in the first step only produced **2a** in 1% yield through such a two-step one-pot process (entry 7, Table 2), suggesting the critically important role of $CuCl_2$ in the photocatalytic degradation of PS. Moreover, heating the

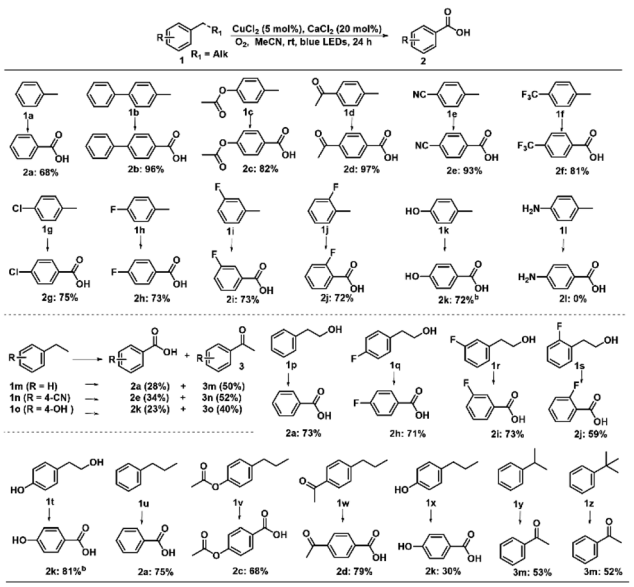


Scheme 2 Substrate scope for the photooxidation of alkylarenes. [a]Reaction conditions: substrate (0.1 mmol), $CuCl_2$ (5 mol%), $CaCl_2$ (20 mol%), MeCN (1.0 mL), $O_2$ balloon, blue LEDs, rt, 24 h. The yields were measured by HPLC using a standard curve of standards as a reference. [b]72 h.

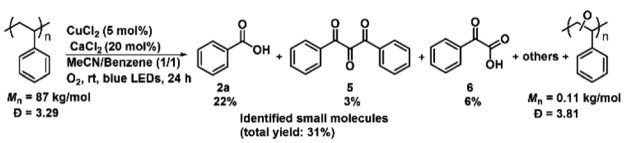


Scheme 3 Results for the PS photooxidative degradation by $CuCl_2$. Reaction conditions: commercial PS (0.1 mmol, based on the amounts of styrene monomer), $CuCl_2$ (5 mol%), $CaCl_2$ (20 mol%), MeCN/benzene (0.6 mL), $O_2$ balloon, blue LEDs, rt, 24 h. The yields were measured by HPLC using a standard curve of standards as reference.

Table 2 Optimization of the two-step one-pot oxidation of PS[a]

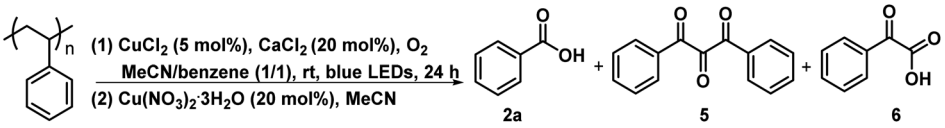


| | First step | | | Second step | | | Yield[b] (%) | | |
|---|---|---|---|---|---|---|---|---|---|
| Entry | Cu-catalyst | *hν* | Time (h) | Catalyst | *T* (°C) | Time (h) | **2a** | **5** | **6** |
| 1 | $CuCl_2/CaCl_2$ | *hν* | 24 | — | — | — | 22 | 3 | 6 |
| 2 | $CuCl_2/CaCl_2$ | *hν* | 36 | — | — | — | 23 | 2 | 6 |
| 3 | $CuCl_2/CaCl_2$ | *hν* | 24 | — | 120 | 12 | 22 | 3 | 5 |
| 4[c] | $CuCl_2/CaCl_2$ | *hν* | 24 | $Cu(NO_3)_2\cdot 3H_2O$ | *hν* | 12 | 22 | 1 | 4 |
| 5 | $CuCl_2/CaCl_2$ | *hν* | 24 | $Cu(NO_3)_2\cdot 3H_2O$ | 120 | 12 | 37 | 0 | 3 |
| 6 | $CuCl_2/CaCl_2$ | *hν* | 24 | $Cu(NO_3)_2\cdot 3H_2O$ | 120 | 24 | 42 | 0 | 2 |
| 7[d] | $Cu(NO_3)_2\cdot 3H_2O/CaCl_2$ | *hν* | 24 | $Cu(NO_3)_2\cdot 3H_2O$ | 120 | 12 | 1 | 0 | 4 |
| 8 | $CuCl_2/CaCl_2$ | *hν* | 24 | $Cu(NO_3)_2\cdot 3H_2O$ | 140 | 24 | 65 | 0 | 0 |
| 9 | $CuCl_2/CaCl_2$ | *hν* | 24 | $Cu(NO_3)_2\cdot 3H_2O$ | 160 | 24 | 51 | 0 | 0 |
| 10[e] | $CuCl_2/Cu(NO_3)_2\cdot 3H_2O/CaCl_2$ | *hν* | 24 | — | 140 | 24 | <1 | 0 | 4 |
| 11[f] | $CuCl_2/Cu(NO_3)_2\cdot 3H_2O/CaCl_2$ | *hν* | — | — | 140 | 24 | <1 | 0 | 0 |

[a] Reaction condition: first step: commercial PS (0.1 mmol, based on the mole amount of the styrene monomer), $CuCl_2$ (5 mol%), $CaCl_2$ (20 mol%), MeCN/benzene (1/1, 0.6 mL), $O_2$ balloon, blue LEDs, rt. Second step: $Cu(NO_3)_2\cdot 3H_2O$ (20 mol%), MeCN (1 mL) was added to the mixture obtained after first step. [b] The yields were measured by HPLC using standard curve of standards as reference. [c] Second step, blue LEDs. [d] $Cu(NO_3)_2\cdot 3H_2O/CaCl_2$ in first step. [e] $CuCl_2/Cu(NO_3)_2\cdot 3H_2O/CaCl_2$ in first step. [f] $CuCl_2/Cu(NO_3)_2\cdot 3H_2O/CaCl_2$ for one-step under blue-LED irradiation at 140 °C.

reaction at 140 °C for 24 h can further increase the yield of **2a** to 65%, while the higher temperature (160 °C) led to a yield decrease to 51% (entries 8 and 9, Table 2). After adding $Cu(NO_3)_2\cdot 3H_2O$ to $CuCl_2/CaCl_2$, the mixture was irradiated for 24 h and then heated at 140 °C for 24 h, only furnishing **2a** in <1% yield, even the irradiating the reaction at 140 °C still could not produce **2a** (entries 10 and 11, Table 2). These results demonstrated that the presence of $Cu(NO_3)_2\cdot 3H_2O$ in the first step would inhibit the reaction. Therefore, the reaction conditions were optimized as the following: $CuCl_2/CaCl_2$ as catalysts under irradiation for 24 h in the first step and $Cu(NO_3)_2\cdot 3H_2O$ at 140 °C for 24 h in the second step.

## Mechanistic studies

**Capture of the radical intermediate.** To gain more insights towards the mechanism of the $CuCl_2$-catalyzed photooxidative degradation of PS, we tried to capture the radical intermediate for this reaction. The addition of the radical scavenger, 2,2,6,6-tetramethylpiperidine-1-oxyl (TEMPO), can completely inhibit the formation of benzoic acid (Scheme S3a†), confirming that this oxidation reaction is a radical reaction. In order to identify the radical intermediate, we utilized propylbenzene as a model substrate to react with one equivalent of $CuCl_2$ in $N_2$ atmosphere, followed by the addition of TEMPO to the reaction mixture. The high-resolution mass spectrometry (HRMS) analysis confirmed the capture of both chlorine and aliphatic radicals by TEMPO (Scheme S3b†).

**Identification of copper active species.** To identify the copper active species for this photocatalytic system, the time-dependent UV-vis absorption spectra were obtained for the mixture of $CuCl_2$ and $CaCl_2$ with or without PS, respectively (Fig. 1). Without PS, the intensities of the characteristic absorption peaks (460 and 310 nm) assigned to the $Cu^{II}Cl_3^-$ gradually decreased to almost zero with the irradiation time (Fig. 1A). The consumption of $Cu^{II}Cl_3^-$ should be attributed to the formation of the reducing $Cu^{I}Cl_2^-$ and chlorine radical *via* a LMCT process.[56–60] The presence of PS would result in an obvious change in the time-dependent UV-vis spectral behaviour of $Cu^{II}Cl_3^-$ (Fig. 1B). In the first 60 min, an absorption peak appeared which was attributed to the gradual weakening of $Cu^{II}Cl_3^-$, indicating the formation of $Cu^{I}Cl_2^-$ and chlorine radical under the irradiation. After 90–150 min, we did not observe the absorption signal of $Cu^{I}Cl_2^-$ but a new absorption band attributed to $Cu^{II}$-OH complexes at 460 nm,[70] probably resulting from the homolysis of the Cu(II)-alkylperoxy complex generated from the reaction of Cu(I) and alkylperoxy radicals (*vide infra*).[71]

To verify the generation of alkoxy radicals from the homolysis of Cu(II)-alkylperoxy complexes, we selected the secondary

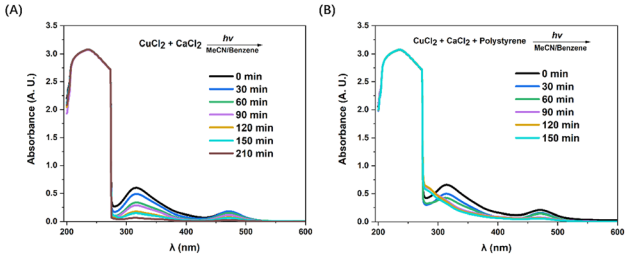


Fig. 1 The time-dependent UV-vis absorption spectra obtained for (A) the mixture of $CuCl_2/CaCl_2$ and (B) the mixture of $CuCl_2/CaCl_2$ with PS.

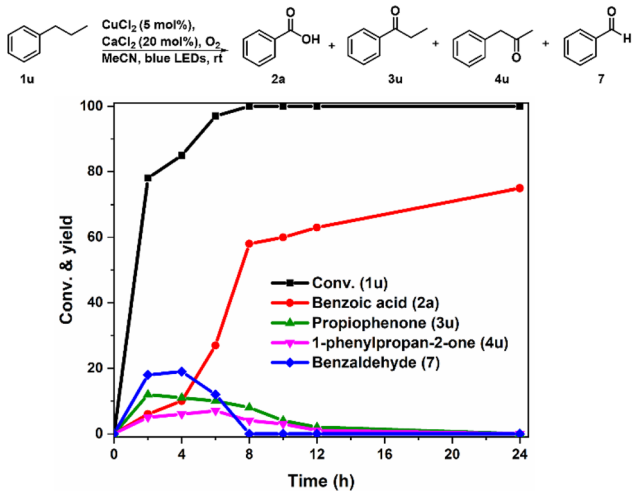


Fig. 2 Time-on-course process of propylbenzene (**1u**) photocatalyzed by $CuCl_2$.

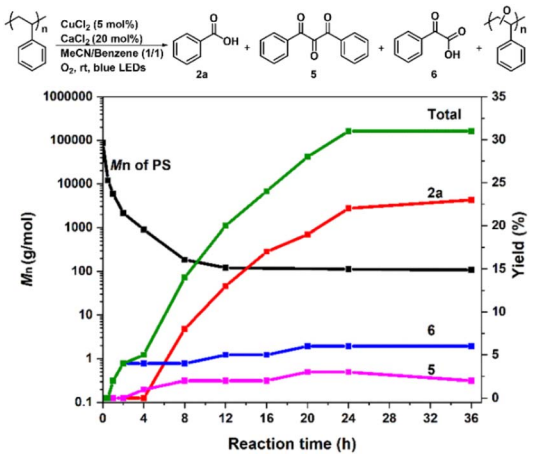


Fig. 3 The time-evolution experiments of $CuCl_2$-catalyzed PS photooxidative degradation (black: $M_n$ of PS; red: yield of **2a**; blue: yield of **6**; pink: yield of **5**; and green: total yield).

propylbenzene (**1u**) as a substrate to detect the direct cleavage product of the C–C bond, which is different from the previously reported carbonyl (C=O) products *via* the aerobic oxidation of secondary sp3 carbon ($-CH_2-$).[36,44] Therefore, the time-on-course oxidation process of **1u** by $CuCl_2$ was monitored by HPLC (Fig. 2). In the first 2 h, benzoic acid (**2a**), propiophenone (**3u**), 1-phenylpropan-2-one (**4u**) and benzaldehyde (**7**) could be detected. The amounts of **3u**, **4u**, and **7** then decreased to zero over time, while the yield of **2a** gradually increased to be the only product ultimately. It should be noted that benzaldehyde (**7**) might be formed during the β-scission of alkoxy radicals generated from the homolysis of O–O bond in the peroxy moiety of the Cu(II)-alkylperoxy complex, which is consistent with the observation for the $Cu^{II}$-OH complex in time-dependent UV-vis spectra (Fig. 1B). Besides, **3u** and **7** were formed after abstracting the benzylic C–H from propylbenzene, while the formation of **4u** confirmed the abstraction of the aliphatic C–H bond.

**Photocatalytic degradation of PS.** To gain deeper insight into the $CuCl_2$-catalyzed photooxidative PS degradation, we also monitored the degradation of PS and formation of small molecular products (Fig. 3 and S6†). The number-average molecular weight ($M_n$) of PS was rapidly decreased from 8.70 $\times 10^4$ to 902 g mol$^{-1}$ in the first 4 h, indicating the generation of oxidized oligomers, 1,3-diphenylpropanetrione (**5**) and phenylglyoxylic acid (**6**) resulting from the cleavage of C–C bond on the PS backbone. From 4 to 24 h, the molecular weight of PS kept decreasing from 902 to 112 g mol$^{-1}$, while the yields of **5** and **6** did not change a lot. Meanwhile, the yield of benzoic acid (**2a**) gradually increased, suggesting that **2a** was produced from the cleavage of the chain-end from the oxidized oligomers.[39] From 24 to 36 h, the yield of **2a** remained almost the same, indicating that there was no transformation of the oligomers into **2a**. To investigate the effect of $M_n$ of polystyrene on the radical reactivity, we also monitored the degradation of PS with different $M_n$ values and found that the benzoic acid formation rate from the PS with low $M_n$ was slightly faster than that from the PS with high $M_n$ (Fig. S7†). These results shed lights on the complicate dynamics of PS degradation and the evolving formation of small molecular products.

**Simulation of polymer chain-end cleavage by using small molecular substrates.** Considering that **2a** was generated from the cleavage of chain-end of the oxidized oligomers (Fig. 3), for simplifying the analysis and better understanding the cleavage process of polymer chain-end, we utilized small molecular reactions to simulate such a process. A series of small molecules were employed as substrates and examined under the standard photocatalytic conditions (Table 3). Using 1,3-diphenylpropane (**8**) as a styrene dimer model substrate produced the targeted C–C bond cleavage products benzoic acid (**2a**), oxidized 1,3-diphenylpropanetrione (**5**) and phenylglyoxylic acid (**6**) in 82%, 2% and 7% yields, respectively (entry 1, Table 3). To probe more insights towards the formation process of C–C bond cleavage products, we monitored the reaction of **8** under standard conditions by $^1$H NMR spectroscopy (Fig. S8†) and found that benzaldehyde (**7**), 1,3-diphenylpropan-1-one (**9**) and 1,3-diphenylpropan-2-one (**10**) were rapidly generated at the initial stage. The formation of **9** was the dominant process, which was decreased along with the generation of **2a**. Control experiments using **9** or **10** as substrates could efficiently produce **2a** (entries 2 and 3, Table 3). Furthermore, kinetic studies revealed that the oxidative C–C cleavage of aromatic ketone **9** was higher priority because the conversion of **9** was faster than that of **10** (Fig. S9 and S10†). All these results indicated that both **9** and **10** are important reaction intermediates. During the monitoring process, small amounts of 1,3-diphenylpropane-1,3-dione (**11**), 2-chloro-1,3-diphenylpropane-1,3-dione (**12**) and 1,3-diphenylpropanetrione (**5**) were observed as the further oxidation products from **9**, which all could be transformed into **2a** ultimately by this photocatalytic system (entries 4–6, Table 3). As there are two pathways to obtain **2a** from **9**: the oxidative C–C cleavage of benzylic carbon in **9** (red pathway) or oxidation of its benzylic C–H bonds into ketone intermediates (**11**, **12** and **5**) followed by the oxidative C–C cleavage of ketones (blue pathway). We

Table 3 Mechanistic studies by using small molecules as substrates[a]

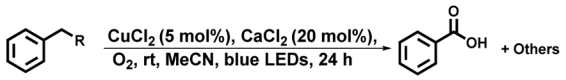


| Entry | Substrate | Conv. | Main products (yield, %) | Entry | Substrate | Conv. | Main products (yield, %) |
|---|---|---|---|---|---|---|---|
| 1 | 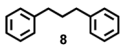 | 100% | 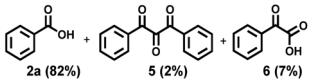 | 7 |  | 34% |  |
| 2 | 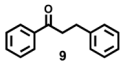 | 100% | 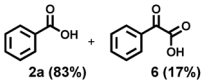 | 8[c] |  | 100% |  |
| 3[b] | 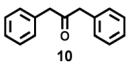 | 100% |  | 9 |  | 100% | 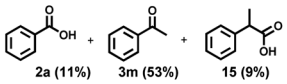 |
| 4 | 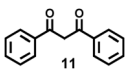 | 100% |  | 10 |  | 100% | 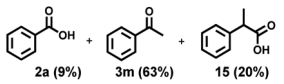 |
| 5 | 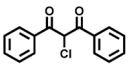 | 100% |  | 11 |  | 26% | 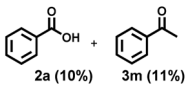 |
| 6 | 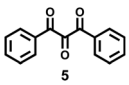 | 100% |  | 12[c] |  | 100% | 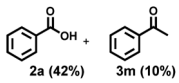 |

[a] Reaction conditions: substrate (0.1 mmol), $CuCl_2$ (5 mol%), $CaCl_2$ (20 mol%), MeCN (1.0 mL), $O_2$ balloon, blue LEDs, rt, 24 h; conversion and yields were measured by HPLC using a standard curve of standards as reference. [b] Blue LEDs, 48 h. [c] Substrate (0.1 mmol), $Cu(NO_3)_2 \cdot 3H_2O$ (20 mol%), MeCN (1.0 mL), 140 °C, 24 h.

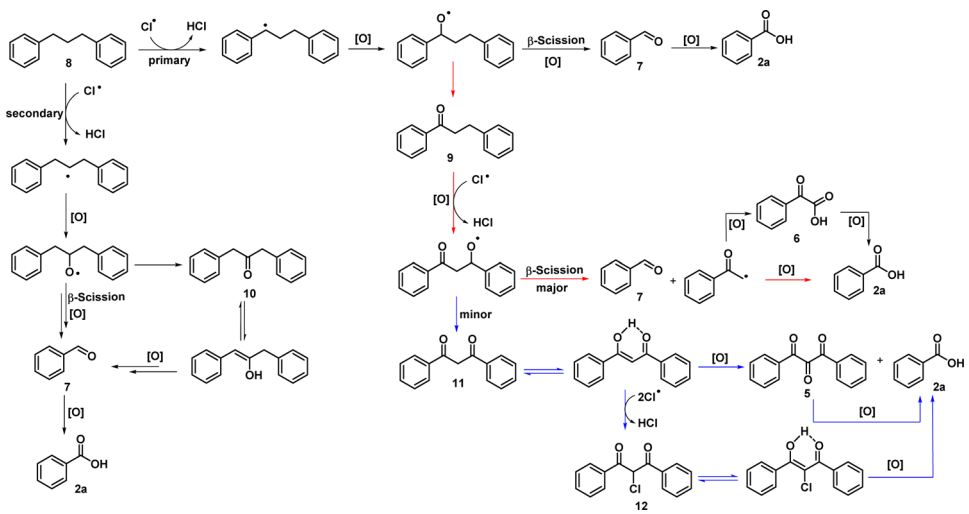


Scheme 4 Possible reaction mechanism proposed for the oxidative C–C bond cleavage of 1,3-diphenylpropane (**8**).

performed a kinetic study of **11** to see which one was preferred and found that the formation rate of **2a** from **11** was really slow (Fig. S11†). In combination with the fact that the ketone intermediates **11** and **12** did not accumulate during the monitoring process, it can be concluded that the oxidative C–C cleavage pathway of **9** was adopted as a major pathway to produce **2a** (red pathway). On the basis of the above results, the proposed mechanism for the conversion of **8** was shown in Scheme 4. Moreover, small amounts of phenylglyoxylic acid (**6**) were detected from the reactions of **8** and **9** under photocatalytic conditions (entries 1–2, Table 3), whereas the yield of **6** from the oxidative degradation of polystyrene in a two-step method was

almost negligible, as the low yield of **2a** was obtained from **6** under photocatalytic conditions, but a high yield of **2a** was obtained from **6** in the presence of $Cu(NO_3)_2 \cdot 3H_2O$ at 140 °C (entries 7 and 8, Table 3). The employment of 2-phenyl-1-propanol (**13**) or 2-phenylpropionaldehy-de (**14**) as the multi-step oxidation model intermediates of alkyl radical chain-ends generated from one oxidative cleavage of PS chain, both furnished the decarbonylation product, acetophenone (**3m**), as a major product along with **2a** and 2-phenylpropionic acid (**15**) as minor products (entries 9 and 10, Table 3). Under photocatalytic conditions, only 34% conversion of **15** and a total 21% yield of cleavage products were obtained (entry 11, Table 3). However, replacing $CuCl_2$ with $Cu(NO_3)_2 \cdot 3H_2O$ and heating at 140 °C can quantitatively convert **15** to **2a** and **3m** in 42% and 10% yield, respectively (entry 12, Table 3). The above results highlighted the fact that both the $Cu(NO_3)_2 \cdot 3H_2O$ catalyst and heating conditions are essentially important for further transformation of the oligomers into the C–C bond cleavage products. The ketone and carboxylic acid moieties are assumed to be installed when primary alcohols and aldehydes are formed on the polymer chain end.

On the basis of the above-described experimental details and previous $CuCl_2$-catalyzed photochemical studies,[54] a plausible reaction mechanism was proposed, as depicted in Scheme 5. First, the chloride of $CaCl_2$ was coordinated with the $Cu^{II}Cl_2$ (**A**) to form photoactive $Cu^{II}Cl_3^-$ (**B**), which can be confirmed by UV-vis spectroscopy (Fig. S5†). Subsequently, the irradiation of $Cu^{II}Cl_3^-$ (**B**) would undergo the LMCT process to generate a reactive chlorine radical (Cl˙) and $[Cu^{I}Cl_2^-]$.[58–60] Due to the stronger bond dissociation (BDE = 103 kcal $mol^{-1}$) compared with that of C–H bond, the Cl˙ could abstract a hydrogen atom from PS (**C**) to generate a carbon-centred radical **D** along with HCl. Radical **D** was then captured by $O_2$ to form a peroxy radical intermediate **E**, which was reduced by $Cu^{I}Cl_2^-$ to generate the $Cl_2Cu$(II)-alkylperoxy complex (**F**).[71] Followed by the O–O bond homolysis of the peroxy moiety, complex **F** was transformed into an alkoxy radical **G** and generate $Cl_2Cu^{II}O$˙.[70,72,73] The $Cl_2$-$Cu^{II}O$˙ complex may abstract a hydrogen from PS other than MeCN solvent[70] because the bond dissociation energy of the benzylic C–H bond (BDE = −90 kcal $mol^{-1}$) is lower than that of the $C_\alpha$–H bond (BDE = 96 kcal $mol^{-1}$)[74] of MeCN, thus transforming **C** into radical **D** and form [$Cl_2Cu^{II}$-OH] complex. Its combination with HCl would close the photocatalytic cycle, along with the release of water. For the selectivity of abstraction of tertiary benzylic C–H or secondary aliphatic C–H *via* Cl˙, we propose two plausible reaction pathways for PS degradation (Scheme 5a and b). Upon the abstraction of tertiary benzylic C–H in PS and subsequent oxidation with $O_2$ (Scheme 5a), the alkoxy radical **G** was generated through the repeated O–O bond homolysis, followed by rapid β-chain cleavage to form an aromatic ketone chain end (**H**) and a primary alkyl radical chain end (**I**). For aromatic ketone chain end **H**, the chlorine radical would abstract a $C_\beta$–H bond adjacent to the ketone to generate a benzylic radical, which was then transformed into the alkoxy radical **J** *via* a repeated oxidation process.[34] The β-chain scission of **J** produced the aromatic ketone chain end **K** and α-acyl radical **L**. The α-acyl radical **L** was oxidized into an oxygen-centred radical by $O_2$, which subsequently underwent β-

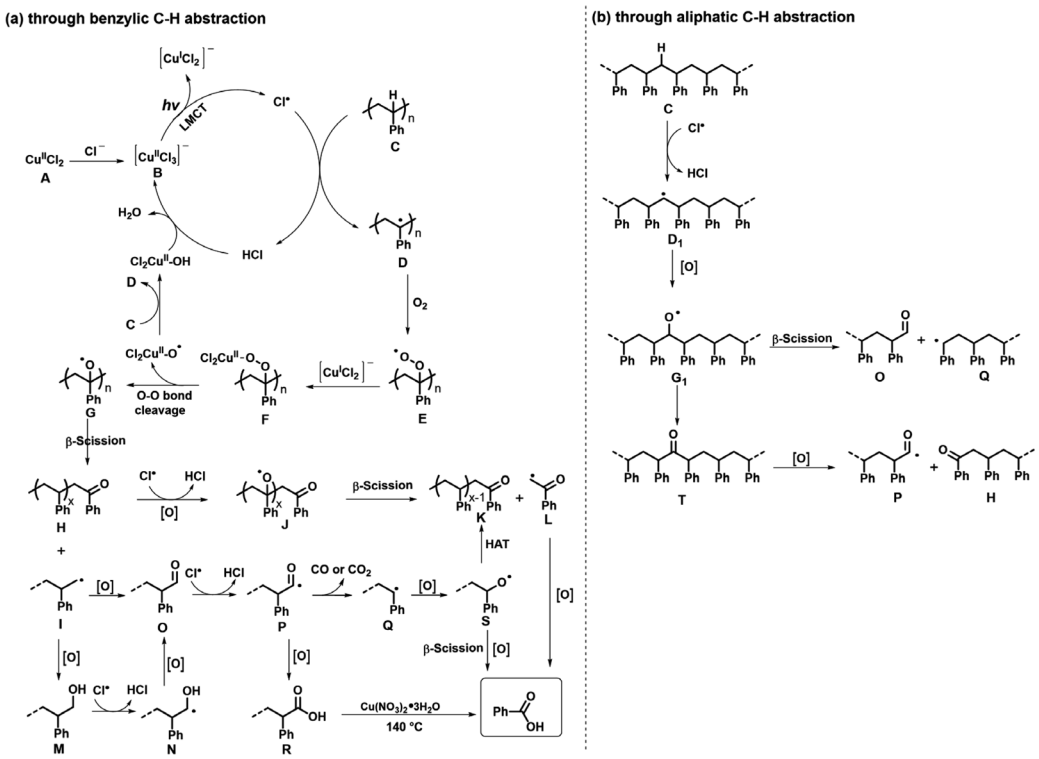


Scheme 5 Possible mechanism proposed for PS degradation through (a) benzylic C–H abstraction or (b) aliphatic C–H abstraction.

scission and oxidation, furnishing benzoic acid ultimately.[39] The primary alkyl radical chain end (**I**) proceeded with the following routes for production of small molecules: First, the chain end **I** could be oxidized to the primary alcohol chain end (**M**) or aldehyde chain end (**O**). The $C_\alpha$–H on the alcohol of **M** can be abstracted by a chlorine radical to form intermediate **N**, which would be rapidly oxidized to aldehyde chain end (**O**).[39] The acyl hydrogen on the aldehyde of **O** could be abstracted to form an acyl radical chain end (**P**) through another HAT. **P** could be decarbonylated to a secondary benzylic radical chain end (**Q**) or partially oxidized to a carboxylic acid moieties chain end (**R**). The chain end **Q** was trapped by $O_2$ to form alkoxy radical chain end (**S**) through repeated O–O bond homolysis, followed by the formation of a ketone chain end **K** *via* HAT or benzoic acid *via* β-chain scission and oxidation processes.

Alternatively, another degradation mechanism occurred through the abstraction of secondary aliphatic C–H bond (Scheme 5b). The reaction involving the secondary C–H abstraction and subsequent oxidation with $O_2$ would generate the secondary alkoxy radical on the PS backbone ($\mathbf{G_1}$), followed by rapid β-chain cleavage to form aldehyde chain end (**O**) and benzylic radical chain end (**Q**).[39] Besides, the secondary alkoxy radical $\mathbf{G_1}$ could also undergo HAT process to produce ketones on the PS backbone (**T**),[44] which would subsequently be oxidized to generate the acyl radical chain end (**P**) and aromatic ketone chain end (**H**). These chain ends (**O**, **Q**, **P**, and **H**) would go through similar processes as above to generate benzoic acid and carboxylic acid moieties chain end (**R**). On the basis of the above-described small molecule study, low conversion of the carboxylic acid moieties chain end (**R**) occurred during photocatalytic process. The fact that full consumption of 2-phenylpropionic acid (**15**) and improved product yield of benzoic acid can be obtained by $Cu(NO_3)_2 \cdot 3H_2O$ under heating conditions (entry 12, Table 3), which also confirmed that the integrated two-step strategy can produce benzoic acid with high efficiency.

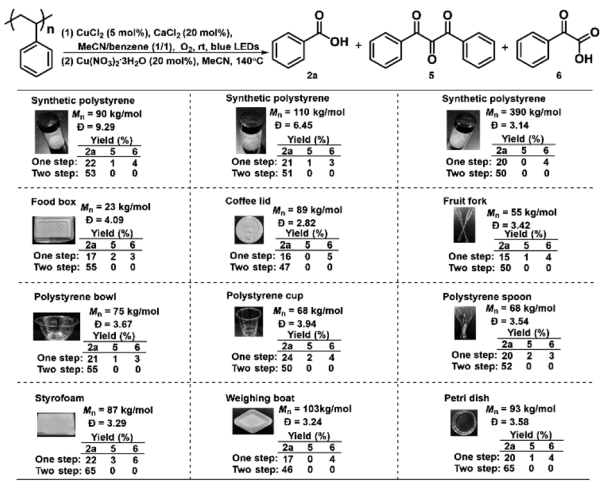


Scheme 6 The degradation of real-life plastic waste. Reaction condition: first step: commercial PS (0.1 mmol, based on the mole amount of the styrene monomer), $CuCl_2$ (5 mol%), $CaCl_2$ (20 mol%), MeCN/Benzene (0.6 mL), $O_2$ balloon, blue LED (50 W), rt, 24 h. Second step: $Cu(NO_3)_2 \cdot 3H_2O$ (20 mol%), MeCN (1 mL) was added to the mixture obtained after first step, 140 °C, 24 h. The average values were obtained from the HPLC yields of two parallel PS degradation experiments.

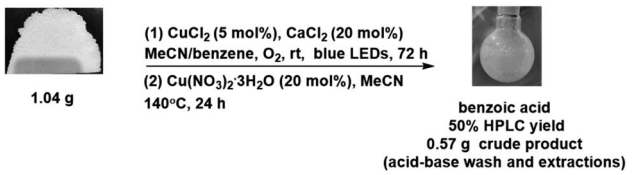


Scheme 7 The gram-scale PS degradation.

With the understanding of the reaction mechanism and optimized reaction conditions at hand, we applied this integrated two-step strategy to a plethora of real-life plastic waste to examine the generality of this strategy (Scheme 6). Initially, the "one step" photocatalytic protocol showed somewhat different effects on the degradation of synthetic PS with different molecular weights, furnishing benzoic acid in 20–22% yields. It is known that polymer additives are typically mixed into real-life PS plastics during their manufacturing. We are very glad to see that this photocatalytic method displayed excellent compatibility with a wide variety of real-life PS waste ranging from food boxes, coffee lids, forks, bowls, cups, spoons, and foam to laboratory weighing boats and Petri dishes, delivering benzoic acid in 15–24% yields. Furthermore, the integrated two-step strategy was adopted to deconstruct PS waste as shown in the "two step". Gratifyingly, the two-step method works well for the degradation of all PS materials, drastically increasing the yield of benzoic acid to 46–65%. There are many additives in commercial polystyrenes, so we selected several widely used polystyrene additives to further investigate the tolerance of our system, such as antioxidants (*e.g.* 2,6-di-*tert*-butyl-*p*-cresol (BHT) and propyl gallate), ultraviolet absorbers (*e.g.* phenyl salicylate and 2-(2-hydroxy-5-methylphenyl)benzotriazole) and 2,4-dihydroxybenzophenone, foaming agents *e.g.* azodicarbonamide and 2,2-azobis(2-methylpropionitrile) and diethyl azodicarboxylate. It turned out that the employment of 0.5 wt% additives did not affect the **2a** yields obtained by our one step photocatalytic protocol and the two-step method, while increasing to 5 wt% additives led to a slight decrease in the **2a** yields, except that 2-(2-hydroxy-5-methylphenyl)benzotriazole showed drastically decreased reactivity *via* a two-step method (Tables S3 and S4†). These results clearly demonstrated the universality and tolerance of the oxidative strategy for recycling PS waste. We also performed a gram-scale degradation of PS waste and obtained benzoic acid in 50% yield (0.57 g after acid–base wash and extractions without further purification), demonstrating the practicality and scalability of this integrated two-step strategy in PS degradation (Scheme 7).

## Conclusions

In summary, we developed a highly efficient photocatalytic strategy for the oxidative cleavage of alkylarenes and

degradation of real-life PS waste into benzoic acid and oxidized styrene oligomers, by using commercially available $CuCl_2$ and $CaCl_2$ as catalysts in $O_2$ atmosphere at room temperature. The addition of $Cu(NO_3)_2 \cdot 3H_2O$ and heating the reaction can further convert the oxidized styrene oligomers to benzoic acid, thus achieving up to 65% total yield of benzoic acid. The practicality and scalability of such a two-step protocol can be verified by the degradation of real-life PS foam on the gram scale, thus showing the great application potentials of this strategy in the recycling of plastic waste into valuable chemicals in the future.

## Data availability

The data supporting the findings of this article have been uploaded as the ESI,† and include full experimental details, NMR and HPLC spectra, and GPC traces.

## Author contributions

E. X. and Y. Z. conceived and designed the experiments. E. X. performed the experiments and characterizations. E. X., T. L., F. X., J. H., and Y. Z. analyzed the data and wrote the manuscript with input from all other authors. Y. Z. directed the projects.

## Conflicts of interest

The authors declare no competing financial interest.

## Acknowledgements

This work was supported by the National Natural Science Foundation of China (grant no. 22225104, 22071077, 21975102, 22471092).

## Notes and references

1 A. Rahimi and J. M. García, *Nat. Rev. Chem.*, 2017, **1**, 0046.
2 M. MacLeod, H. P. H. Arp, M. B. Tekman and A. Jahnke, *Science*, 2021, **373**, 61–65.
3 S. R. Nicholson, N. A. Rorrer, A. C. Carpenter and G. T. Beckham, *Joule*, 2021, **5**, 673–686.
4 J. R. Jambeck, R. Geyer, C. Wilcox, T. R. Siegler, M. Perryman, A. Andrady, R. Narayan and K. L. Law, *Science*, 2015, **347**, 768–771.
5 H. Ran, S. Zhang, W. Ni and Y. Jing, *Chem. Sci.*, 2024, **15**, 795–831.
6 T. Tan, W. Wang, K. Zhang, Z. Zhan, W. Deng, Q. Zhang and Y. Wang, *ChemSusChem*, 2022, **15**, e202200522.
7 M. Q. Zhang, M. Wang, B. Sun, C. Hu, D. Xiao and D. Ma, *Chem*, 2022, **8**, 2912–2923.
8 Z. Ouyang, Y. Yang, C. Zhang, S. Zhu, L. Qin, W. Wang, D. He, Y. Zhou, H. Luo and F. Qin, *J. Mater. Chem. A*, 2021, **9**, 13402–13441.
9 C. W. S. Yeung, J. Y. Q. Teo, X. J. Loh and J. Y. C. Lim, *ACS Mater. Lett.*, 2021, **3**, 1660–1676.
10 A. J. Martín, C. Mondelli, S. D. Jaydev and J. Pérez-Ramírez, *Chem*, 2021, **7**, 1487–1533.
11 C. Jehanno, J. W. Alty, M. Roosen, S. De Meester, A. P. Dove, E. Y. X. Chen, F. A. Leibfarth and H. Sardon, *Nature*, 2022, **603**, 803–814.
12 D. Kwon, *Nature*, 2023, **616**, 234.
13 L. Gan, Z. W. Dong, H. F. Xu, H. D. Lv, G. X. Liu, F. Zhang and Z. Huang, *CCS Chem.*, 2024, **6**, 313.
14 B. Zhao, H. Tan, J. Yang, X. Zhang, Z. Yu, H. Sun, J. Wei, X. Zhao, Y. Zhang, L. Chen, D. Yang, J. Deng, Y. Fu, Z. Huang and N. Jiao, *The Innovation*, 2024, **5**, 100586.
15 X. Jia, C. Qin, T. Friedberger, Z. Guan and Z. Huang, *Sci. Adv.*, 2016, **2**, e1501591.
16 C. Marquez, C. Martin, N. Linares and D. De Vos, *Mater. Horiz.*, 2023, **10**, 1625–1640.
17 J. C. Capricho, K. Prasad, N. Hameed, M. Nikzad and N. Salim, *Polymers*, 2022, **14**, 5010.
18 L. D. Ellis, N. A. Rorrer, K. P. Sullivan, M. Otto, J. E. McGeehan, Y. Román-Leshkov, N. Wierckx and G. T. Beckham, *Nat. Catal.*, 2021, **4**, 539–556.
19 J. M. Garcia and M. L. Robertson, *Science*, 2017, **358**, 870–872.
20 A. C. Albertsson and M. Hakkarainen, *Science*, 2017, **358**, 872–873.
21 B. Singh and N. Sharma, *Polym. Degrad. Stab.*, 2008, **93**, 561–584.
22 W. Partenheimer, *Catal. Today*, 2003, **81**, 117–135.
23 K. P. Sullivan, A. Z. Werner, K. J. Ramirez, L. D. Ellis, J. R. Bussard, B. A. Black, D. G. Brandner, F. Bratti, B. L. Buss, X. Dong, S. J. Haugen, M. A. Ingraham, M. O. Konev, W. E. Michener, J. Miscall, I. Pardo, S. P. Woodworth, A. M. Guss, Y. Román-Leshkov, S. S. Stahl and G. T. Beckham, *Science*, 2022, **378**, 207–211.
24 C. Rabot, Y. Chen, S. Y. Lin, B. Miller, Y. M. Chiang, C. E. Oakley, B. R. Oakley, C. C. C. Wang and T. J. Williams, *J. Am. Chem. Soc.*, 2023, **145**, 5222–5230.
25 X. Luo, J. Zhan, Q. Mei and S. Zhang, *Green Chem.*, 2023, **25**, 6717–6727.
26 Y. Jing, Y. Wang, S. Furukawa, J. Xia, C. Sun, M. J. Hülsey, H. Wang, Y. Guo, X. Liu and N. Yan, *Angew. Chem., Int. Ed.*, 2021, **60**, 5527–5535.
27 C. Qin, T. Shen, C. H. Tang and N. Jiao, *Angew. Chem., Int. Ed.*, 2012, **51**, 6971–6975.
28 N. E. Munyaneza, C. Posada, Z. Xu, V. De Altin Popiolek, G. Paddock, C. McKee and G. Liu, *Angew. Chem., Int. Ed.*, 2023, **62**, e202307042.
29 J. Kou, C. Lu, J. Wang, Y. Chen, Z. Xu and R. S. Varma, *Chem. Rev.*, 2017, **117**, 1445–1514.
30 S. Chu, B. Zhang, X. Zhao, H. S. Soo, F. Wang, R. Xiao and H. Zhang, *Adv. Energy Mater.*, 2022, **12**, 2200435.
31 F. Eisenreich, *Angew. Chem., Int. Ed.*, 2023, **62**, e202301303.
32 Y. Zhang, M. Y. Qi, Z. R. Tang and Y. J. Xu, *ACS Catal.*, 2023, **13**, 3575–3590.
33 E. Skolia, O. G. Mountanea and C. G. Kokotos, *Trends Chem.*, 2023, **5**, 116–120.
34 E. Yousif and R. Haddad, *SpringerPlus*, 2013, **2**, 398.
35 J. Shang, M. Chai and Y. Zhu, *Environ. Sci. Technol.*, 2003, **37**, 4494–4499.

36 M. Wang, J. Wen, Y. Huang and P. Hu, *ChemSusChem*, 2021, **14**, 5049–5056.
37 G. Zhang, Z. Zhang and R. Zeng, *Chin. J. Chem.*, 2021, **39**, 3225–3230.
38 S. Oh and E. E. Stache, *J. Am. Chem. Soc.*, 2022, **144**, 5745–5749.
39 S. Oh and E. E. Stache, *ACS Catal.*, 2023, **13**, 10968–10975.
40 A. Ong, Z. C. Wong, K. L. O. Chin, W. W. Loh, M. H. Chua, S. J. Ang and J. Y. C. Lim, *Chem. Sci.*, 2024, **15**, 1061–1067.
41 Z. Huang, M. Shanmugam, Z. Liu, A. Brookfield, E. L. Bennett, R. Guan, D. E. Vega Herrera, J. A. Lopez-Sanchez, A. G. Slater, E. J. L. McInnes, X. Qi and J. Xiao, *J. Am. Chem. Soc.*, 2022, **144**, 6532–6542.
42 S. Xu, S. Liu, W. Song and N. Zheng, *Green Chem.*, 2024, **26**, 1363–1369.
43 R. Cao, M. Q. Zhang, C. Hu, D. Xiao, M. Wang and D. Ma, *Nat. Commun.*, 2022, **13**, 4809.
44 T. Li, A. Vijeta, C. Casadevall, A. S. Gentleman, T. Euser and E. Reisner, *ACS Catal.*, 2022, **12**, 8155–8163.
45 N. F. Nikitas, E. Skolia, P. L. Gkizis, I. Triandafillidi and C. G. Kokotos, *Green Chem.*, 2023, **25**, 4750–4759.
46 Y. Qin, T. Zhang, H. Y. V. Ching, G. S. Raman and S. Das, *Chem*, 2022, **8**, 2472–2484.
47 C. Li, X. Y. Kong, M. Lyu, X. T. Tay, M. Đokić, K. F. Chin, C. T. Yang, E. K. X. Lee, J. Zhang, C. Y. Tham, W. X. Chan, W. J. Lee, T. T. Lim, A. Goto, M. B. Sullivan and H. S. Soo, *Chem*, 2023, **9**, 2683–2700.
48 J. Meng, Y. Zhou, D. Li and X. Jiang, *Sci. Bull.*, 2023, **68**, 1522–1530.
49 A. Hossain, A. Bhattacharyya and O. Reiser, *Science*, 2019, **364**, 450.
50 Q. Y. Li, S. N. Gockel, G. A. Lutovsky, K. S. DeGlopper, N. J. Baldwin, M. W. Bundesmann, J. W. Tucker, S. W. Bagley and T. P. Yoon, *Nat. Chem.*, 2022, **14**, 94–99.
51 Y. Li, K. Zhou, Z. Wen, S. Cao, X. Shen, M. Lei and L. Gong, *J. Am. Chem. Soc.*, 2018, **140**, 15850–15858.
52 V. P. Charpe, A. Sagadevan and K. C. Hwang, *Green Chem.*, 2020, **22**, 4426–4432.
53 A. Hossain, A. Vidyasagar, C. Eichinger, C. Lankes, J. Phan, J. Rehbein and O. Reiser, *Angew. Chem., Int. Ed.*, 2018, **57**, 8288–8292.
54 A. S. Mereshchenko, P. K. Olshin, A. M. Karimov, M. Y. Skripkin, K. A. Burkov, Y. S. Tveryanovich and A. N. Tarnovsky, *Chem. Phys. Lett.*, 2014, **615**, 105–110.
55 C. Meng, K. Yang, X. Fu and R. Yuan, *ACS Catal.*, 2015, **5**, 3760–3766.
56 K. Takaki, J. Yamamoto, K. Komeyama, T. Kawabata and K. Takehira, *Bull. Chem. Soc. Jpn.*, 2004, **77**, 2251–2255.
57 K. Takaki, J. Yamamoto, Y. Matsushita, H. Morii, T. Shishido and K. Takehira, *Bull. Chem. Soc. Jpn.*, 2003, **76**, 393–398.
58 J. K. Kochi, *J. Am. Chem. Soc.*, 1962, **84**, 2121–2127.
59 P. Lian, W. Long, J. Li, Y. Zheng and X. Wan, *Angew. Chem., Int. Ed.*, 2020, **59**, 23603–23608.
60 S. M. Treacy and T. Rovis, *J. Am. Chem. Soc.*, 2021, **143**, 2729–2735.
61 A. A. Fokin and P. R. Schreiner, *Chem. Rev.*, 2002, **102**, 1551–1594.
62 X. P. Zhang, A. Chandra, Y. M. Lee, R. Cao, K. Ray and W. Nam, *Chem. Soc. Rev.*, 2021, **50**, 4804–4811.
63 C. García-Sancho, I. Fúnez-Núñez, R. Moreno-Tost, J. Santamaría-González, E. Pérez-Inestrosa, J. L. G. Fierro and P. Maireles-Torres, *Appl. Catal., B*, 2017, **206**, 617–625.
64 C. Lin, H. Wu, V. Wang, J. Huang, F. Cao, W. Zhuang, Y. Lu, J. Chen, H. Jia and P. Ouyang, *Ind. Eng. Chem. Res.*, 2020, **59**, 4358–4366.
65 C. Lin, C. Chai, Y. Li, J. Chen, Y. Lu, H. Wu, L. Zhao, F. Cao, K. Chen, P. Wei and P. Ouyang, *Green Chem.*, 2021, **23**, 2058–2068.
66 P. G. David and P. A. C. da Silva, *Bull. Chem. Soc. Jpn.*, 1985, **58**, 3566–3569.
67 R. Chinchilla and C. Nájera, *Chem. Soc. Rev.*, 2011, **40**, 5084–5121.
68 L. Lopez, L. Troisi, S. M. K. Rashid and A. P. Schaap, *Tetrahedron Lett.*, 1989, **30**, 485–488.
69 H. Liu, M. Wang, H. Li, N. Luo, S. Xu and F. Wang, *J. Catal.*, 2017, **346**, 170–179.
70 T. Tano, M. Z. Ertem, S. Yamaguchi, A. Kunishita, H. Sugimoto, N. Fujieda, T. Ogura, C. J. Cramer and S. Itoh, *Dalton Trans.*, 2011, **40**, 10326–10336.
71 H. R. Lucas, L. Li, A. A. N. Sarjeant, M. A. Vance, E. I. Solomon and K. D. Karlin, *J. Am. Chem. Soc.*, 2009, **131**, 3230–3245.
72 A. Kunishita, H. Ishimaru, S. Nakashima, T. Ogura and S. Itoh, *J. Am. Chem. Soc.*, 2008, **130**, 4244–4245.
73 B. Kim, D. Jeong and J. Cho, *Chem. Commun.*, 2017, **53**, 9328–9331.
74 L. Tanwar, J. Börgel and T. Ritter, *J. Am. Chem. Soc.*, 2019, **141**, 17983–17988.